Plant Physiology and Biochemistry 143 (2019) 320–328

Contents lists available at ScienceDirect

Plant Physiology and Biochemistry

journal homepage: www.elsevier.com/locate/plaphy

Research article

proline content alterative 17 (*pca17*) is involved in glucose response through sulfate metabolism-mediated pathway

Tinh Van Nguyen[a], Moon-Soo Chung[b], Jung-Sung Chung[c], Cheol Soo Kim[a,*]

[a] Department of Applied Biology, Chonnam National University, Gwangju, 61186, Republic of Korea
[b] Research Division for Biotechnology, Advanced Radiation Technology Institute, Korea Atomic Energy Research Institute, Jeongeup-si, Jeollabuk-do, 56212, Republic of Korea
[c] Department of Agronomy, Gyeongsang National University, Jinju, 660-701, Republic of Korea

ARTICLE INFO

Keywords:
AHL
AMP
atrzf1
pca17
Cysteine
Glucose
Sulfate metabolism

ABSTRACT

Sulfate metabolism and glucose (Glc) signaling are important processes required for plant growth, development, and environmental responses. However, whether sulfate metabolism is involved in *Arabidopsis* response to Glc stress remains largely unclear. Recently, we have found that *proline content alterative 17* (*pca17*) is a double-mutant line in which both *AtRZF1* (for *Arabidopsis thaliana Ring Zinc Finger 1*) and *AHL* (for *Arabidopsis Halotolerance 2-like*) genes are mutated. It was found that insensitive response of *atrzf1* mutant to abiotic stresses was suppressed in *pca17* mutant by regulating proline metabolism. Here, *pca17* appeared to have sensitive response to Glc treatment by reducing cysteine (Cys) and adenosine monophosphate (AMP) contents in sulfate metabolism. Under Glc treatment, transcript levels of sulfate metabolism-related genes were significantly lower in *pca17* than those in wild-type (WT) and *atrzf1*. Furthermore, *AHL*-overexpressing transgenic lines displayed more insensitive phenotypes than WT during Glc condition while *ahl* RNAi lines exhibited sensitive responses based on several parameters, including seed germination rate, cotyledon greening percentage, root elongation, and fresh weight. Interestingly, the *pca17* phenotype in applied AMP with Glc treatment was similar to *atrzf1* phenotype. Taken together, our results indicate that AHL is involved in Glc response by modulating sulfate metabolism in *Arabidopsis*.

1. Introduction

Sulfur is one of essential macronutrient components required for plant growth and development. In nature, sulfate is the most abundant form of sulfur that can be taken up by plants. The components of primary sulfate metabolism have been discovered. However, how can they regulate plant underlying response to disadvantageous environment remains largely unclear. Cysteine (Cys) is a first organic compound of primary sulfate metabolism (Takahashi et al., 2011). Cys is an amino acid for protein construction in plants. It is also a precursor for a large number of essential biomolecules such as vitamins, cofactors, and Fe–S group (Romero et al., 2014). Moreover, Cys derivatives can form abundant important bio-components including glutathione, methionine, glucosinolates, and camalexin (Romero et al., 2014). Sulfur-containing metabolites are known to be necessary for various aspects of plant development, growth, and unfavorable environmental response. As an example of such metabolites, glutathione (GSH) is an antioxidant that plays an important role in cellular redox homeostasis regulated by thiol group including Cys (Noctor et al., 2012). Besides, GSH can contribute to plant response to adverse environment such as detoxification of heavy metal and xenobiotic (Dixon et al., 2002; Mendoza-Cozatl et al., 2011; Rea, 2012). Interestingly, increasing cytosolic Cys accumulation can confer tolerance of plant to cadmium stress (Dominguez-Solis et al., 2004; Romero et al., 2014).

Secondary sulfate metabolism such as 3′-phosphoadenosine-5′-phosphosulfate (PAPS) branch has been less understood. Adenosine monophosphate (AMP) in secondary sulfate metabolism is a byproduct of 3′-phosphoadenosine-5′-phosphate (PAP) catalyzed by 3' (2′), 5′-bisphosphate nucleotidase or PAP phosphatase (Chen et al., 2011; Estavillo et al., 2011). AMP is a monomer of RNA production and a component in many metabolic processes. However, whether AMP is involved in environmental response remains unclear. AHL (for *Arabidopsis* Halotolerance 2-like) is a PAP phosphatase that shares more than 40% amino acid sequence identities with the SAL (for SAL phosphatase-

Abbreviations: AMP, adenosine monophosphate; qPCR, quantitative real-time polymerase chain reaction; RT-PCR, reverse transcription-PCR; WT, wild-type

* Corresponding author.
E-mail address: cskim626@jnu.ac.kr (C.S. Kim).

https://doi.org/10.1016/j.plaphy.2019.09.019
Received 27 April 2019; Received in revised form 10 August 2019; Accepted 13 September 2019
Available online 14 September 2019
0981-9428/ © 2019 Elsevier Masson SAS. All rights reserved.

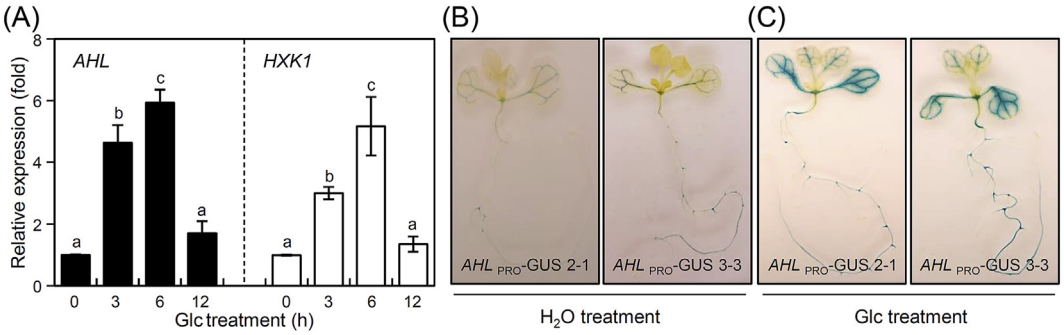

Fig. 1. Expression of *AHL* in *Arabidopsis* seedlings or *AHL* $_{PRO}$-GUS transgenic plants under Glc condition. (A) Expression levels of *AHL* and *HXK1* involved in Glc response by qPCR. All quantifications were made using three independently extracted total RNA samples that were obtained from 14-day-old *Arabidopsis* seedlings treated without or with 6% Glc at indicated time. Error bars indicate standard deviations of triplicate independent experiments (n = 10, ANOVA, $P < 0.05$). Different letters above bars indicate statistically significant difference. *Arabidopsis Actin 1* was as an internal control. (B) GUS expression pattern of transgenic lines (*AHL* $_{PRO}$-GUS 2–1 and 3-3) with H_2O or 10% Glc for 12 h. Tests were repeated three times with similar results.

like) family (Chen et al., 2011; Shin et al., 2019). AHL might not directly participate in PAP accumulation under stress conditions (Chen et al., 2011; Shin et al., 2019). In fact, loss of *AHL* in *pca17* (for *proline content alterative 17*) mutant leads to decreased PAP content under osmotic stress possibly due to SAL1 activity (Shin et al., 2019). Besides, AMP level in *pca17* is lower than that in WT or *atrzf1* (for *Arabidopsis thaliana ring zinc finger 1*) during osmotic stress (Shin et al., 2019), suggesting that AHL is required for AMP biosynthesis in *Arabidopsis*.

In plants, glucose (Glc) is fundamental to various metabolic processes, including germination, early seedling growth, root and leaf differentiation, flowering time, and senescence (Rolland et al., 2006). Furthermore, exogenous Glc can affect expression of various genes in *Arabidopsis* seedling (Price et al., 2004). Microarray analysis results have shown that Glc biosynthesis and signaling in plants are closely associated with abscisic acid (ABA) (Li et al., 2006). In *Arabidopsis*, Hexokinase 1 (HXK1) is an enzyme that catalyzes phosphorylation of sucrose at the first step of glycolytic pathway. HXK1 was discovered as a Glc sensor (Graham et al., 1994; Jang et al., 1997). Indeed, HXK1 can mediate Glc signaling by controlling seedling development that involves increased expressions of both ABA synthesis and signaling genes (Rolland et al., 2006). Exogenous Glc can increase ABA level in young seedlings (Arenas-Huertero et al., 2000; Cheng et al., 2002) and suppress seed germination in *Arabidopsis* (Price et al., 2004). In addition, exogenous Glc can enhance sulfur assimilation in which induction of sulfate metabolism-related genes and accumulations of Cys and GSH levels are evident (Miao et al., 2016). However, regulation of sulfate metabolism-related genes involved in Glc response remains unclear.

E3 ubiquitin ligase AtRZF1 could regulate dehydration, ABA, and oxidative stress by modulating Pro biosynthesis factors and ABA signaling response genes (Kim et al., 2017; Shin et al., 2019). The *pca17* was generated by T-DNA tagging mutagenesis of *atrzf1* parental mutant. Physiological phenotypes of *pca17* including germination and cotyledon greening rates exhibited more sensitive responses under abiotic stress than those of WT and *atrzf1* parental mutant, suggesting that the insensitivity of *atrzf1* under abiotic stress was suppressed in *pca17* (Shin et al., 2019). Interestingly, accumulation of AMP in *pca17* is lower than that in WT or *atrzf1* (Shin et al., 2019). Therefore, AHL might have a role in AMP reduction in *Arabidopsis* under abiotic stress (Shin et al., 2019).

We wonder whether AHL might be able to regulate primary sulfate metabolism under Glc stress. To gain insight to this, the current work evaluated the function of AHL in Glc response by studying sulfate metabolisms of WT, *atrzf1*, and *pca17* using genetics, physiological, and molecular biological assays. Obtained results showed that destruction of *AHL* in *pca17* suppressed insensitivity of *atrzf1* phenotype under high Glc concentration. Moreover, contents of Cys and AMP in *pca17* were lower than those in WT and *atrzf1* after Glc treatment. Additionally, Glc-induced sensitive phenotype of *pca17* treated with AMP showed a close to *atrzf1* phenotype, indicating a rescue of *pca17* by exogenously supplied AMP. These observations suggest that AHL plays a role in Glc response by modulating Cys and AMP biosynthesis pathway in *Arabidopsis* seedling.

2. Results

2.1. AHL is upregulated by Glc treatment

The *pca17* is a double mutant in which both *AtRZF1* and *AHL* genes are mutated. AHL is a PAP phosphatase involved in secondary sulfate metabolism. Our previous data have shown that AHL can regulate responses to abiotic stresses including mannitol, ABA, and hydroperoxide treatments (Shin et al., 2019). Additionally, sulfur assimilation is regulated by Glc through enhanced mRNA transcripts of both primary and secondary sulfate metabolism-related genes (Miao et al., 2016).

To investigate how Glc treatment might affect the expression level of *AHL* mRNA, 2-week-old *Arabidopsis* plants were subjected to 6% Glc treatment and analyzed with quantitative real-time PCR (qPCR). As shown in Fig. 1A, time-course expression levels of *AHL* gene showed a peak within 6 h after Glc treatment followed by downregulation until 12 h. Glc-inducible marker gene, *HXK1*, was used as a control for Glc treatment (Fig. 1A). This result suggests that *AHL* is regulated by Glc. To gain more insight into tissue specificities of *AHL* expression, we investigated β-glucuronidase (GUS) expression levels in 1925-bp *AHL* promoter-GUS 2–1 and 3-3 transgenic plants (Shin et al., 2019) after treatment without or with Glc. Under Glc-untreated condition, GUS staining was weak in primary root, lateral roots, and leaf vein (Fig. 1B). However, GUS staining of *AHL* promoter-GUS transgenic lines was strong in primary root, lateral roots, hypocotyl-root junction part, and leaf vein under Glc-treated condition (Fig. 1C). These observations indicate that *AHL* is specifically regulated in plant tissue by Glc. To further study the change of *AHL* expression in shoot and root in response to Glc, we examined expression patterns of *AHL* in shoot and root after Glc treatment. As shown in Supplementary Fig. S1A, *AHL* transcripts were increased in shoot than that in root under Glc-treated condition whereas *AHL* was predominantly expressed in the root under normal condition. These results indicate that *AHL* level is altered in response to with or without Glc in the shoot and root.

2.2. Loss of AtRZF1 regulated the level of AHL transcript

Recently, we have found that destruction of *AHL* in *pca17* can lead to suppressed insensitivity of *atrzf1* phenotype under abiotic stress (Shin et al., 2019). To investigate whether *AtRZF1* might affect expression level of *AHL* mRNA, 2-week-old seedlings of WT, *atrzf1*, and

pca17 were subjected to 6% Glc treatment followed by qPCR analysis. As shown in Supplementary Fig. S1B, *AHL* expression in *atrzf1* was increased approximately 5.8-fold compared to that in WT plant after H_2O treatment. When Glc was applied to seedling samples, *AHL* expression levels were significantly induced in both WT and *atrzf1*. *AHL* expression was increased more in *atrzf1* compared to that in WT under Glc condition (Supplementary Fig. S1B). There was no expression of *AHL* in *pca17* regardless whether it was treated with Glc (Supplementary Fig. S1B). This suggests that *AtRZF1* and *AHL* genes are both knocked out in *pca17* mutant. These data demonstrate that *AtRZF1* regulates *AHL* expression. To further confirm whether *AHL* expression could be regulated by *AtRZF1*, accumulation of *AHL* mRNA was assessed in *AtRZF1*-overexpressing line (OX1-1) previously described by Ju et al. (2013) using qPCR (Supplementary Fig. S1B). Interestingly, the transcript of *AHL* gene was lower in *AtRZF1*-overexpressing line (OX1-1) compared to that in WT or *atrzf1* (Supplementary Fig. S1B), implying the expression level of *AHL* gene may be regulated through ubiquitination pathway that is a biochemical function of AtRZF1.

2.3. Glc response of pca17 mutant

Since expression level of *AHL* in *atrzf1* was increased under normal or Glc conditions compared to that in WT (Supplementary Fig. S1B), we investigated phenotypes of WT, *atrzf1*, *pca17*, and complementary (Com4 and Com9) seedlings (Shin et al., 2019) after treatment with 6% Glc. As shown in Supplementary Fig. S2A, germination rates were similar among WT, *atrzf1*, *pca17*, and complementary (Com4 and Com9) plants. They were not diminished in MS (Murashige and Skoog) media. However, at 3–6 days after treatment with Glc, seed germination rate of *pca17* was lower than that of WT, *atrzf1*, or complementary plants (Fig. 2A). In addition, germination rates were similar between *atrzf1* and complementary lines, but higher than those of WT after 3–6 days of exposure to Glc (Fig. 2A). Glc-induced sensitivity was further evaluated by measuring cotyledon greening rate. The relative reduction in cotyledon greening of *pca17* in response to 6% Glc was more intense than that of WT, *atrzf1*, or complementary lines at 12 (Supplementary Fig. S2B and Fig. 2B) or 14 days (Fig. 2B) after seed germination. Cotyledon greening rates of *atrzf1* or complementary lines were higher than those of WT at 12 or 14 days after Glc treatment whereas those of *atrzf1* and complementary lines were nearly similar under high Glc concentration (Fig. 2B). These results suggest that *atrzf1* and complementary lines have more insensitive response of seed germination or cotyledon greening than *pca17* to high Glc concentration.

2.4. Glc response in AHL transgenic plants

To further characterize the role of destructed *AHL* in *pca17* phenotype under Glc condition, we used *AHL*-overexpressing (OE2-2 and OE5-1) and *ahl* RNA interference (RNAi) (*ri2-3* and *ri5-2*) transgenic plants as described previously (Shin et al., 2019). In the absence of Glc, no obvious phenotypic difference was observed among WT, *AHL*-overexpressing, and *ahl* RNAi transgenic plants (Supplementary Fig. S2A). As shown in Fig. 2C and D, under 6% Glc condition, relative germination and cotyledon greening rates were lower in *ahl* RNAi (*ri2-3* and *ri5-2*) lines compared to those in WT and *AHL*-overexpressing (OE2-2 and OE5-1) transgenic lines for seed germination at indicated days or seedlings at same stage (12 or 14 days). However, *AHL*-overexpressing lines displayed higher germination and cotyledon greening rates than WT in the presence of 6% Glc (Fig. 2C and D). These results indicate that AHL is required for Glc-regulated seed germination and cotyledon greening in *Arabidopsis*.

The extent of Glc-induced sensitivity was also assessed by measuring the length of primary root elongation and fresh weight (FW). When seeds of WT, *atrzf1*, *pca17*, *ahl* RNAi (*ri2-3*), *AHL*-overexpressing (OE2-2), and complementary (Com4) lines were germinated on MS agar plate containing 4 or 6% Glc, under the normal condition, the primary root length and FW were similar among WT, mutants, and *AHL* transgenic plants grown on the MS medium (Fig. 3 and Supplementary Fig. S3A). As shown in Fig. 3A and Supplementary Fig. S3B, primary root lengths were similar among WT, *pca17*, and *ri2-3* lines at 4 or 6% Glc. However, primary root lengths of *atrzf1*, OE2-2, and Com4 lines at 4% Glc were 1.4-, 1.3-, and 1.2-fold longer, respectively, compared to that of WT. Similarly, primary root lengths of *atrzf1*, OE2-2, and Com4 lines at 6% Glc were 1.5-, 1.8-, and 1.9-fold longer, respectively, compared to that of WT (Fig. 3A). In addition, the FWs were reduced in *pca17* and *ri2-3* lines, in comparison with FW of WT under 6% Glc condition (Fig. 3B and Supplementary Fig. S3B). However, FWs were significantly higher in *atrzf1*, OE2-2, and Com4 lines than those in WT, *pca17*, and *ri2-3* lines in response to 6% Glc (Fig. 3B). Thus, *atrzf1*, *AHL*-overexpressing, and complementary lines were more insensitive to Glc than WT, *pca17*, and *ahl* RNAi lines. This finding suggests that both AtRZF1 and AHL are most likely to be involved in the regulation of plant growth in response to Glc in *Arabidopsis*.

2.5. Glc-induced hydrogen peroxide (H_2O_2) accumulation is promoted in pca17 mutant

Reactive oxygen species (ROS) are known to regulate root growth by controlling cell differentiation and division (Dunand et al., 2007; Yu et al., 2016). Since *AtRZF1* and *AHL* are involved in the regulation of root growth in response to Glc exposure (Fig. 3A and Supplementary Fig. S3), we examined ROS levels in detached leaves or whole seedlings of WT, *atrzf1*, and *pca17* after Glc treatment. Glc-induced H_2O_2 accumulation was determined by DAB staining. As shown in Supplementary Fig. S4, no significant difference in H_2O_2 distribution pattern was found for detached 5th-leaf and whole seedlings of samples after untreated Glc. Treatment with 15% Glc promoted the accumulation of H_2O_2 in *pca17* detached 5th-leaf and whole seedling. However, detached 5th-leaf and whole seedling of *atrzf1* accumulated lower levels of H_2O_2 than WT and *pca17* under treatment with the same concentration of Glc (Supplementary Fig. S4). This result suggests that ROS signaling is important for the regulation of root growth in *atrzf1* and *pca17* against Glc treatment.

2.6. Analyses of Glc-upregulated genes in pca17

It is relatively well established that transcriptional levels of *HXK1*, *Glucose insensitive 6* (*GIN6*), *Arabidopsis thaliana oxidation-related zinc finger 2* (*AtOZF2*), *Delta 1-pyrroline-5-carboxylate synthase 1* (*P5CS1*), *Abscisic acid responsive elements-binding factor 2* (*ABF2*), *ABA insensitive 5* (*ABI5*), *Arabidopsis thaliana plasma membrane Glc-responsive regulator* (*AtPGR*), and *Arabidopsis thaliana MYB 75* (*MYB75*) are upregulated by Glc or abiotic stress (Strizhov et al., 1997; León and Sheen, 2003; Rolland et al., 2006; Min et al., 2017; Sakr et al., 2018; Shin et al., 2019). To determine whether expression levels of Glc-related genes are responsible for the increased sensitivity to Glc in *pca17*, we quantified *HXK1*, *GIN6*, *AtOZF2*, *P5CS1*, *ABF2*, *ABI5*, *AtPGR*, and *MYB7*5 mRNA levels through qPCR. As shown in Fig. 4, Glc-induced expression levels of *HXK1*, *GIN6*, and *ABI5* mRNAs were increased in *pca17* compared to those in WT and *atrzf1* whereas expression levels of these three genes were less induced in *atrzf1* than those in WT. In contrast, transcription levels of *AtOZF2*, *P5CS1*, *ABF2*, *AtPGR*, and *MYB75* were decreased by Glc treatment in *pca17* compared to those in WT and *atrzf1* while they were induced in *atrzf1* than those in WT. These observations suggest that *pca17* can enhance Glc-induced *HXK1*, *GIN6*, and *ABI5* or suppress Glc-induced *AtOZF2*, *P5CS1*, *ABF2*, *AtPGR*, and *MYB75* expression. Thus, it is possible that AHL can act negatively or positively depending on the signal required for regulating the type of Glc-inducible genes under high Glc condition. For example, PAP is accumulated in chloroplast. It plays a role as retrograde signaling to reduce stress damage under abiotic stress conditions (Estavillo et al., 2011; Pornsiriwong et al., 2017). Additionally, PAP is known as an inhibitor of small

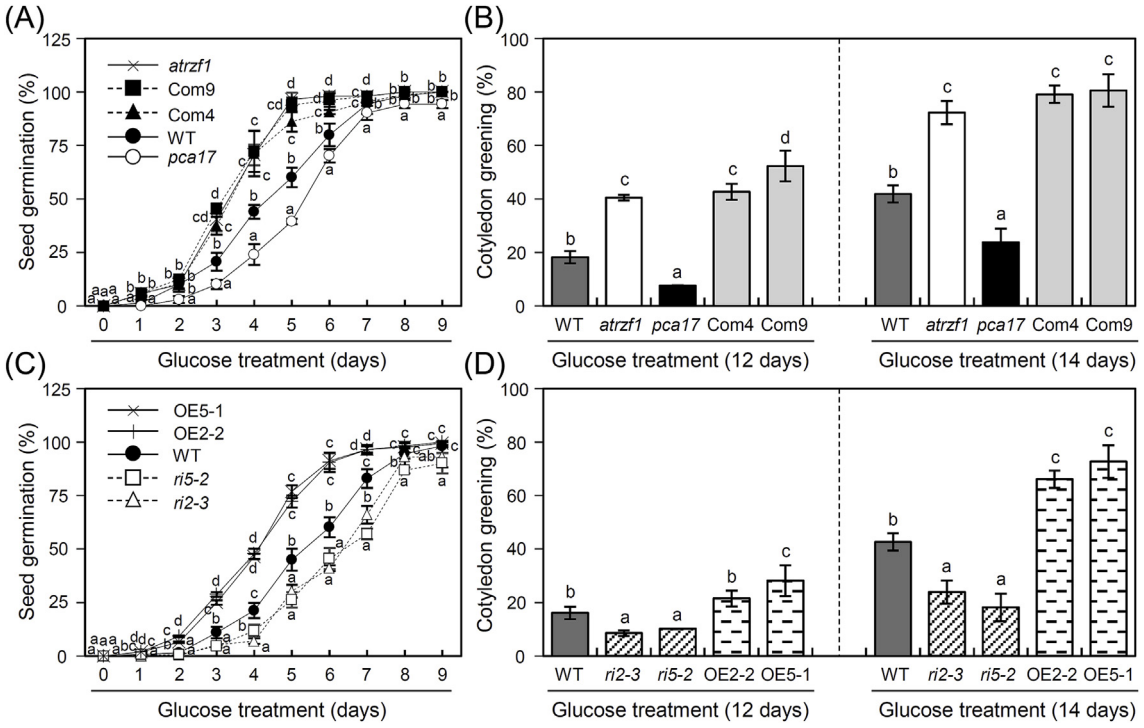

Fig. 2. Inhibition of seed germination and cotyledon greening rates by Glc. (A) Effect of Glc on seed germination. Seeds of WT, *atrzf1*, *pca17*, and complementary (Com4, Com9) plants were sown on MS media supplement with 6% Glc and allowed to germinate for indicated days and then germination was scored. Error bars indicate standard deviations of triplicate independent experiments (n = 50 of each, ANOVA, $P < 0.05$). Different letters above bars indicate statistically significant difference. (B) Effect of Glc on cotyledon greening. Seeds of WT, *atrzf1*, *pca17*, and complementary (Com4, Com9) plants were sown on MS agar plates supplement with 6% Glc and allowed to grow for 12 or 14 days and then seedlings with green cotyledons were scored. Error bars indicate standard deviations of triplicate independent experiments (n = 50 of each, ANOVA, $P < 0.05$). Different letters above bars indicate statistically significant difference. (C) Effect of Glc on seed germination. Seeds of WT, *AHL*-overexpressing (OE2-2, OE5-1), and *ahl* RNAi (*ri2-3*, *ri5-2*) plants were sown on MS agar plates supplement with 6% Glc and allowed to germinate for indicated days and then germination was scored. Error bars indicate standard deviations of triplicate independent experiments (n = 50 of each, ANOVA, $P < 0.05$). Different letters above bars indicate statistically significant difference. (D) Effect of Glc on cotyledon greening. Seeds of WT, *AHL*-overexpressing (OE2-2, OE5-1), and *ahl* RNAi (*ri2-3*, *ri5-2*) plants were sown on MS agar plates supplement with 6% Glc and allowed to grow for 12 or 14 days and then seedlings with green cotyledons were scored. Error bars indicate standard deviations of triplicate independent experiments (n = 50 of each, ANOVA, $P < 0.05$). Different letters above bars indicate statistically significant difference.

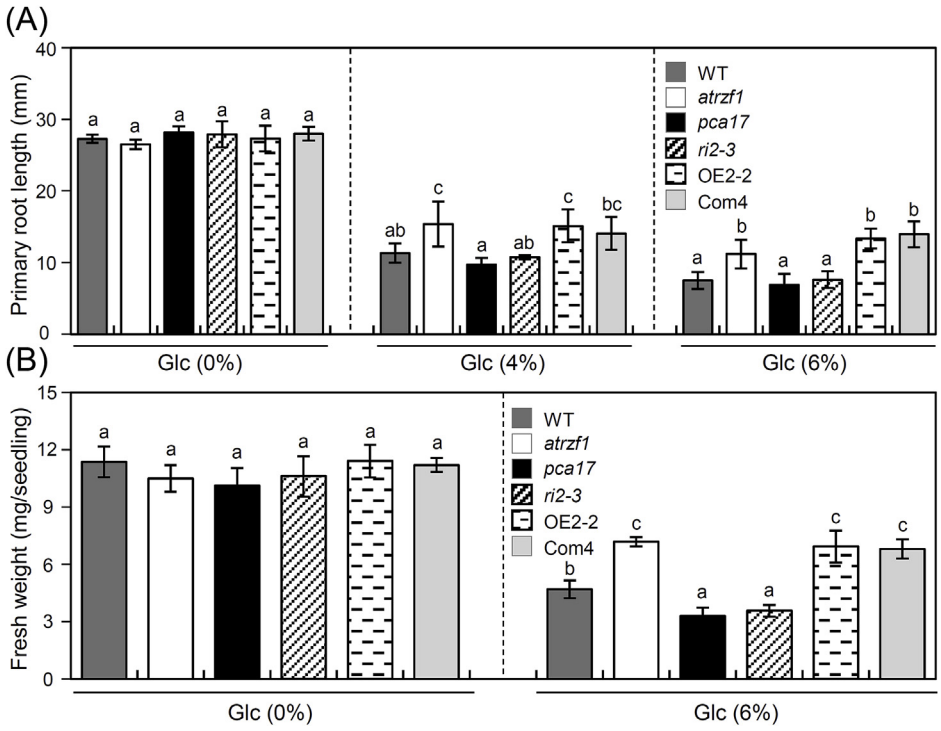

Fig. 3. Inhibition of primary root elongation and fresh weight by Glc. (A) Comparison of primary root lengths of WT, *atrzf1*, *pca17*, *ahl* RNAi (*ri2-3*), *AHL*-overexpressing (OE2-2), and complementary (Com4) plants grown on MS agar plates containing 0, 4, or 6% Glc for 14, 14, or 16 days, respectively. Error bars indicate standard deviations of triplicate independent experiments (n = 25 of each, ANOVA, $P < 0.05$). Different letters above bars indicate statistically significant difference. (B) Effect of Glc on seedling fresh weight. Seeds of WT, *atrzf1*, *pca17*, *ahl* RNAi (*ri2-3*), *AHL*-overexpressing (OE2-2), and complementary (Com4) plants grown on MS agar plates containing 0 or 6% Glc for 16 days. Error bars indicate standard deviations of triplicate independent experiments (n = 25 of each, ANOVA, $P < 0.05$). Different letters above bars indicate statistically significant difference.

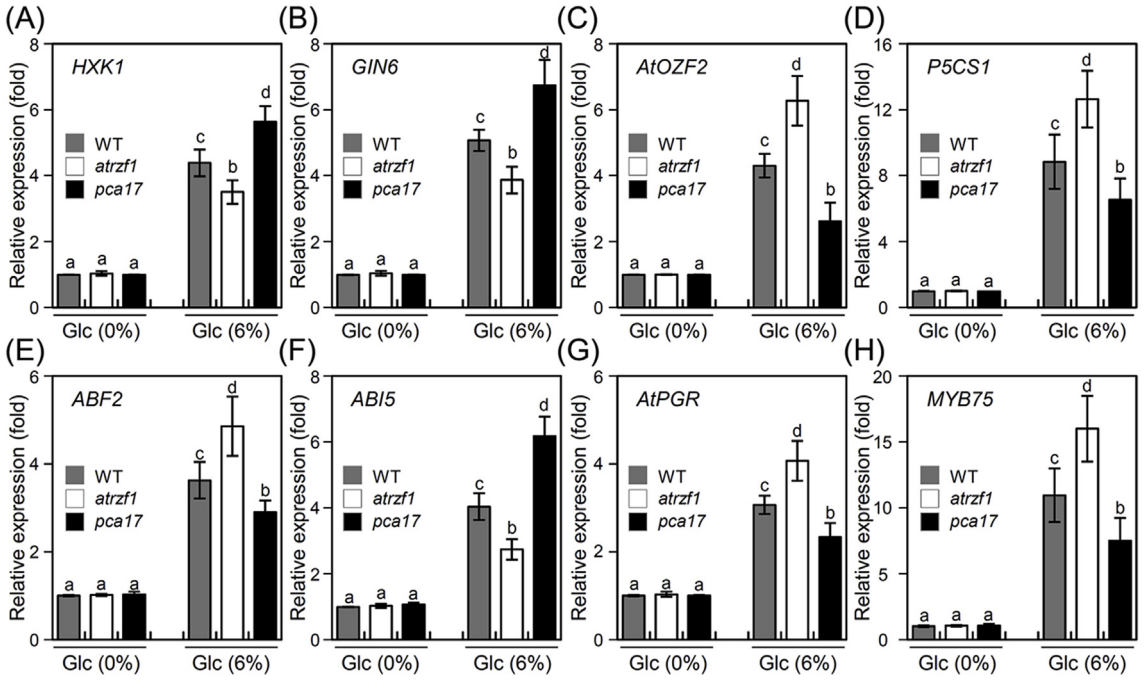

Fig. 4. Expression levels of Glc-responsive genes in WT, *atrzf1*, and *pca17*. (A–D) mRNA levels of *HXK1* (A), *GIN6* (B), *AtOZF2* (C), *P5CS1* (D), *ABF2* (E), *ABI5* (F), *AtPGR* (G), and *MYB75* (H) were analyzed by qPCR using total RNAs extracted from 14-day-old WT, *atrzf1*, and *pca17* plants that were untreated or treated with 6% Glc for 6 h. Error bars indicate standard deviations of triplicate independent experiments (n = 10 of each, ANOVA, $P < 0.05$). *Actin 1* was used as internal control. Different letters above bars indicate statistically significant difference.

interference RNA action by alteration of RNA-metabolizing endoribonuclease enzymes (Estavillo et al., 2011). Therefore, an alternative link between PAP pathway and Glc signaling may involve RNA metabolism corrected by a particular factor. These results reveal that *pca17* mutant participates in Glc sensitive response through *AHL* mutation-mediated Glc signaling.

2.7. Analyses of proline content and sulfate metabolic products in pca17 under Glc condition

Although osmotic stress response of *pca17* has been previously elucidated (Shin et al., 2019), it is of interest to exam the ability of *AHL* mutation in *pca17* to suppress the function of *atrzf1* in Glc response. Thus, we tested proline (Pro), AMP, and Cys contents in rosette leaves of WT, *atrzf1*, and *pca17* in the presence of 0% Glc or 10% Glc. In the absence of Glc treatment, Pro contents were similar among WT, *atrzf1*, and *pca17* (Fig. 5A). In the presence of high concentration of Glc, relative Pro content was higher in *atrzf1* compared to that in WT or *pca17*, although it was lower in *pca17* than that in WT seedlings (Fig. 5A). This observation demonstrates that loss of *AHL* in *atrzf1* can reduce Pro accumulation under high Glc concentration. *AHL* expression is associated with sulfate metabolism (Shin et al., 2019). AMP and Cys contents in WT, *atrzf1*, and *pca17* seedlings were also measured. AMP and Cys productions were induced by Glc treatment (Fig. 5B and C). As shown in Fig. 5B and C, AMP and Cys contents were higher in *atrzf1* than those in WT and *pca17*, although it was lower in *pca17* than that in WT in the presence or absence of high Glc concentration. These results suggest that *pca17* can suppress the synthesis of not only AMP in secondary sulfate pathway, but also Cys in primary sulfate metabolism under normal and high Glc conditions. In addition, Glc can enhance the accumulation of sulfate metabolic products.

2.8. Transcript accumulation of sulfate metabolism-related genes in pca17 and AHL transgenic plants

To evaluate sulfate metabolism in *pca17* and *AHL* transgenic plants at molecular level, transcript levels of *Adenosine triphosphate sulfurylase 1* (*ATPS1*), *Arabidopsis thaliana PAPS reductase 1* (*AtAPR1*), *AtAPR2*, *AtAPR3*, *Sulfite reductase* (*SiR*), *O-Acetylserine thiol lyase 1* (*OASA1*), *Adenosine-5′-phosphosulfate kinase 1* (*APK1*), *APK2*, and *Sulfotransferase 2A* (*ST2A*) known to increase in response to Glc (Miao et al., 2016) were measured using qPCR (Fig. 6). Transcript levels of Glc-inducible genes, including *ATPS1*, *AtAPR2*, *AtAPR3*, *SiR*, *OASA1*, *APK1*, and *ST2A*, were increased more in *atrzf1* and *AHL*-overexpressing OE2-2 plants than those in WT, *pca17*, and *ahl* RNAi (*ri 2–3*) plants after Glc treatment. However, transcript levels of these seven genes were lower in *pca17* and *ri2-3* lines than those in WT seedlings, although the accumulation of these seven genes were similar between *pca17* and *ri2-3* lines under Glc condition (Fig. 6A, 6C-G and 6I). As shown in Fig. 6F, transcript level of *OASA1*, a key cytosolic enzyme generated Cys product (Alvarez et al., 2010), was higher in *atrzf1* and OE2-2 lines than that in WT, *pca17*, or *ri2-3* line under normal condition. However, the transcript level of this gene was lower in *pca17* and *ri2-3* lines than that in WT. These results suggest that molecular events of primary or secondary pathway of sulfate metabolism-related genes are decreased more in *pca17* and *ahl* RNAi plants than those in *atrzf1* and *AHL*-overexpressing plants. Thus, AHL can regulate the expression of AtRZF1-mediated sulfate metabolism-related genes under Glc condition. Although high expression levels of *AtAPR1* and *APK2* genes observed in *atrzf1* under Glc condition, the accumulation of these two genes in WT, *pca17*, and *AHL* transgenic plants seem to be very similar (Fig. 6B and H). This probably suggests that the overexpression or disruption of *AHL* by itself is not sufficient for the regulation of *AtAPR1* and *APK2* genes and may require additional molecules under Glc condition.

2.9. AMP and Cys modulate Glc-induced inhibition of cotyledon greening

Because sulfate metabolic products were lower in *pca17* compared to those in WT and *atrzf1* (Fig. 5B and C), we tested whether Glc-induced sensitive phenotype of *pca17* could be rescued after treatment with AMP or Cys. To characterize effect of AMP or Cys on Glc response, we analyzed cotyledon greening of WT, *atrzf1*, and *pca17* in the

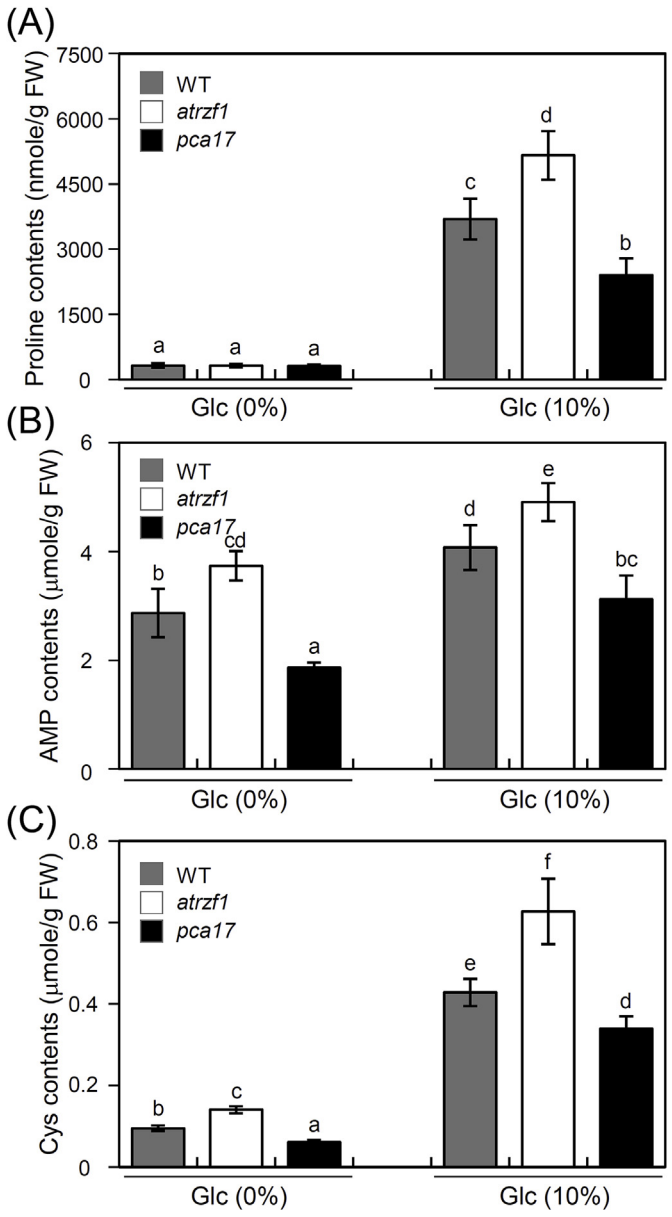

Fig. 5. Analyses of Pro, AMP, and Cys concentrations in WT, *atrzf1*, and *pca17*. Leaves of 5-week-old WT, *atrzf1*, and *pca17* plants were treated with or without 10% Glc for 12 h. Values of Pro (A), AMP (B), and Cys contents (C) describe the average of triplicate independent experiments (n = 10 of each, error bars ± SD, ANOVA, $P < 0.05$). Different letters above bars indicate statistically significant difference.

presence of AMP (20 μM), Cys (40 μM), or both under Glc condition. Under Glc condition, seedlings treated with these components showed higher cotyledon greening efficiency than untreated samples (Fig. 7 and Supplementary Fig. S4). This result suggests that AMP and Cys can modulate Glc-induced inhibition of cotyledon greening. As shown in Fig. 7, when only AMP or AMP combined with Cys was used for treatment, cotyledon greening rates of *pca17* and *atrzf1* mutants nearly were not significantly different under Glc, although they were higher than those of WT in response to Glc (Fig. 7). Therefore, AMP is able to rescue Glc-induced early growth defects of *pca17* mutant. When Cys was applied to samples, cotyledon greening rate of *pca17* was higher than that of WT under Glc, but lower than that *atrzf1* in response to Glc (Fig. 7), indicating a partial rescue of *pca17* by Cys treatment. These data indicate an important role of AMP and Cys in Glc-related early growth regulation.

3. Discussion

It has been demonstrated that Glc can regulate sulfate assimilation through SNF1-related protein kinases signaling (Davies et al., 1999). For example, Davies et al. (1999) have reported that *Chlamydomonas* SAC3, a SNF1-like serine threonine kinase, is involved in activating the sulfate transport system under sulfur limitation. SNF1-related protein kinases are known as key components of abiotic stress-response pathways in plants (Coello et al., 2011). Recently, Miao et al. (2016) have demonstrated that Glc plays a positive role in sulfur assimilation. After investigating transcript levels of both primary and secondary sulfate metabolic-related genes induced by Glc signaling, they found that Glc promoted Cys accumulation under sulfate conditions (Miao et al., 2016). Our previously data have shown that AHL can regulate abiotic stress responses, including dehydration, ABA, and oxidative stress (Shin et al., 2019). AHL encodes PAP phosphatase that can catalyze PAP to AMP in secondary sulfate metabolism (Chen et al., 2011). Here, we further investigated whether AHL could regulate underlying sulfate metabolism pathway under Glc condition in *pca17* mutant.

To observe effects of Glc treatment on expression level of *AHL* mRNA, *AHL* expression patterns were analyzed at tissue level under Glc condition using GUS reporter lines and qPCR (Fig. 1 and Supplementary Fig. S1). Generally, *AHL* showed increased expression patterns in the shoot and root under Glc condition (Supplementary Fig. S1A). *AHL* gene had distinct expression patterns in the shoot and root. It was more highly expressed in the shoot compared to that in the root under Glc condition, although *AHL* was highly expressed in the root under normal condition (Supplementary Fig. S1A). Interestingly, *AHL* expression was highly accumulated in *atrzf1* mutant, but weakly in *AtRZF1*-over-expressing line, compared to that in WT after treatment with or without Glc (Supplementary Fig. S1B). This result suggests that *AHL* is regulated by *AtRZF1*-mediated pathway.

It is generally accepted that high Glc can causes delay of germination and inhibit early seedling growth (Price et al., 2004). Indeed, *AHL* mutation in *pca17* can suppress insensitive trait of its parental *atrzf1* under dehydration condition (Shin et al., 2019). Furthermore, as shown in Fig. 2 and Supplementary Fig. S2, the relative inhibition of seed germination or early seedling growth of *pca17* in response to Glc was more intense than that of WT, *atrzf1*, or complementary lines. Thus, *pca17* suppressed insensitive trait of *atrzf1* under Glc condition. This indicates that *AtRZF1* is a negative regulator of *AHL* in response to Glc. Besides, *AHL*-overexpressing transgenic lines showed more insensitive response in seed germination, cotyledon greening, and fresh weight than *ahl* RNAi lines after Glc treatments (Figs. 2 and 3, and Supplementary Fig. S2). These physiological data suggest that both AtRZF1 and AHL are involved in the modulation of early seedling growth against Glc in *Arabidopsis*. These data also showed a distinct difference in expressions of *HXK1*, *GIN6*, *AtOZF2*, *P5CS1*, *ABF2*, *ABI5*, *AtPGR*, and *MYB75* genes between *atrzf1* and *pca17* after treatment with Glc. Fig. 4 shows that *pca17* can enhance Glc-negative regulators *HXK1*, *GIN6*, and *ABI5* expression or suppress Glc-positive regulators *AtOZF2*, *P5CS1*, *ABF2*, *AtPGR*, and *MYB75* expression compared to WT and *atrzf1* after Glc treatment (Strizhov et al., 1997; León and Sheen, 2003; Rolland et al., 2006; Min et al., 2017; Sakr et al., 2018; Shin et al., 2019). Altered transcripts of these Glc-related genes demonstrate that *AHL* can regulate the expression of *AtRZF1*-mediated Glc-responsive genes under Glc condition. Phenotypic analysis of root lengths in WT, *atrzf1*, *pca17*, *AHL* transgenic, and complementary plants indicated that growth of primary root of *pca17* mutant was suppressed compared to root length of *atrzf1* during low or high Glc concentration treatment. In addition, *AHL*-overexpressing and complementary lines showed long-root phenotypes compared to WT and *ahl* RNAi seedlings (Fig. 3A and Supplementary Fig. S3). These results suggest that AHL can function in root growth under Glc condition.

More recently, Sami and Hayat (2019) have demonstrated that Glc application can modulate Pro content and hydrogen peroxide level in

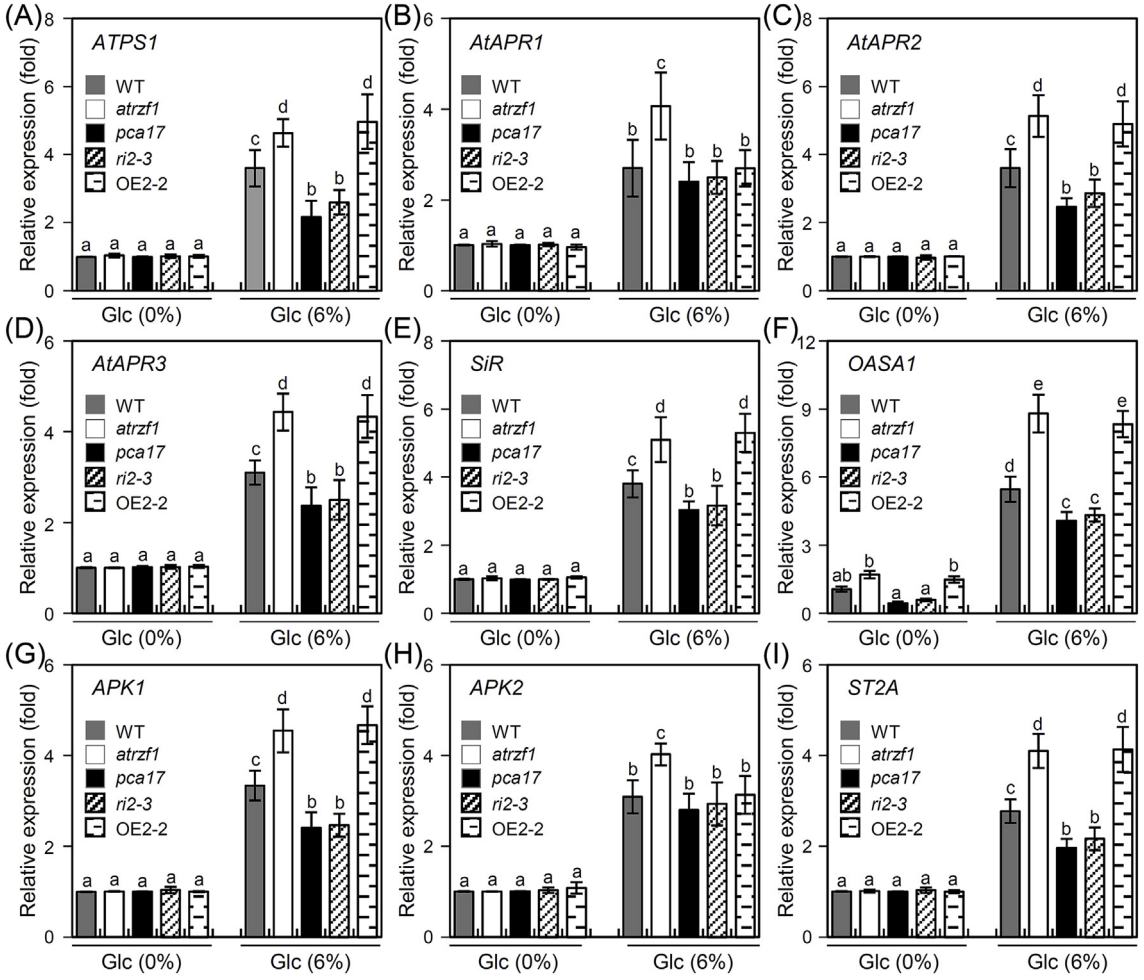

Fig. 6. Transcript profiles for sulfate metabolism-regulated gene in WT, *atrzf1*, *pca17*, and *AHL* transgenic plants after treatment with or without Glc. (A–I) Results provide relative sulfate metabolism-regulated transcript levels and describe the average of triplicate independent experiments (n = 20, error bars ± SD, ANOVA, $P < 0.05$). Different letters above bars indicate statistically significant difference. *Actin 1* was used as internal control. *ATPS1* (A), *AtAPR1* (B), *AtAPR2* (C), *AtAPR3* (D), *SiR* (E), *OASA1* (F), *APK1* (G), *APK2* (H), and *ST2A* (I) mRNA levels were measured by qPCR using total RNAs isolated from 10-day-old WT, *atrzf1*, *pca17*, *ahl* RNAi (*ri2-3*), or *AHL*-overexpressing (OE2-2) seedlings untreated or treated with 6% Glc for 6 h.

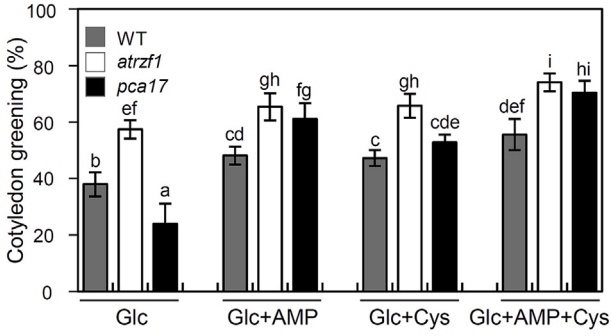

Fig. 7. Responses of cotyledon greening to Glc under AMP or Cys condition. Seeds of WT, *atrzf1*, and *pca17* plants were grown in MS agar plates with 20 μM AMP, 40 μM Cys, or 20 μM AMP combined with 40 μM Cys under 6% Glc condition and permitted to grow for 14 days. Seedlings with green cotyledons were counted. Error bars indicate standard deviations of triplicate independent experiments (n = 50 of each, ANOVA, $P < 0.05$). Different letters above bars indicate statistically significant difference.

Brassica juncea. Pro accumulation in plants can regulate abiotic stress tolerance by adjusting osmotic balance or maintaining cell turgor. Pro can stabilize membranes and prevent electrolyte leakage. Pro also can diminish ROS concentration to assist plant recovery from abiotic stress (Szabados and Savouré, 2010; Hayat et al., 2012; Kim et al., 2017). Our data also showed distinct differences in Pro content and ROS level between *pca17* and *atrzf1* (Fig. 5A and Supplementary Fig. S4). Accumulation of Pro in *pca17* exhibited lower levels while ROS in *pca17* showed higher levels than WT and *atrzf1* after high Glc concentration treatment (Fig. 5A and Supplementary Fig. S4). This implies that AHL is responsible for the reduction of Glc-induced sensitivity through regulation of osmotic balance and ROS production.

It is known that Glc signaling can regulate sulfate assimilation (Davies et al., 1999; Miao et al., 2016). As a precursor or donor of sulfur reduction, Cys is a component for forming a range of sulfur-containing compounds, including methionine, GSH, homo-glutathione, phytochelatins (Anjum et al., 2015). Cys accumulation modulates plant response to biotic stress such as against *Botrytis criteria* infection in *Lycopersicon esculentum* (Kuzniak and Sklodowska, 2005). Cytosolic Cys accumulation is declined in *oasa-1a* mutant triggered sensitivity to cadmium toxin (Dominguez-Solis et al., 2004; Romero et al., 2014). Moreover, Cys is a precursor of GSH which is upregulated in abiotic stress for coordinating Cys and GSH biosynthesis (Chan et al., 2013). In secondary sulfate metabolism, AMP is a byproduct of PAP in reaction catalyzed by SAL or AHL (Chen et al., 2011; Estavillo et al., 2011). AMP is a monomer of RNA synthesis that participates in various cellular metabolic processes. Recently, we have reported that loss of *AHL* in *pca17* causes declined levels of Pro, PAP, and AMP, leading to

suppression of insensitive phenotype of its parental *atrzf1* under dehydration condition (Shin et al., 2019). The accumulation of AMP and Cys is regulated by Glc treatment in *atrzf1* and *pca17* mutants (Fig. 5B and C), implying that AtRZF1 and AHL can link sulfate metabolism in a Glc-dependent pathway. To determine this possibility, transcript levels of various sulfate metabolism-related genes (*ATPS1*, *AtAPR1*, *AtAPR2*, *AtAPR3*, *SiR*, *OASA1*, *APK1*, *APK2*, and *ST2A*) were measured in WT, *atrzf1*, *pca17*, and *AHL* transgenic seedlings without or with Glc treatment. Fig. 6 shows that disruption of *AHL* functions in *pca17* or *ahl* RNAi line can lead to reduced transcription of both primary and secondary of several sulfate metabolism-related genes. This result suggests that AHL positively regulates these sulfate metabolism-related genes. We have previously reported that *APK1* and *APK2* genes are expressed in both *atrzf1* and *pca17* mutants similar to that in WT after the application of mannitol, indicating that *atrzf1* and *pca17* mutants do not affect their dehydration response to *APKs* expressions (Shin et al., 2019). In contrast, transcript level of *APK1* displayed enhanced reduction in *pca17* and *ahl* RNAi lines compared with WT, *atrzf1*, and *AHL*-overexpressing plants following Glc treatment, whereas expression level of *APK2* in WT, *pca17*, *ahl* RNAi, and *AHL*-overexpressing plants under Glc condition seemed to be very similar (Fig. 6G and H). Thus, the reduced expression of *APK1*, but not *APK2*, by *AHL* upon apply to exogenous Glc might provide evidence that AHL participates in Glc response through an APK1-mediated sulfate metabolism pathway. Therefore, AHL might be important components in Glc dependent-regulated sulfate metabolism products or that they can indirectly exert effects on sulfate metabolism. Additionally, exogenously applied AMP can rescue Glc-induced sensitive phenotype of *pca17* while Cys treatment can lead to partial rescue of phenotype of *pca17* (Fig. 7 and Supplementary Fig. S5). These data indicate that *pca17*-sensitive phenotype to Glc response is mainly dependent on AMP. These findings indicate that sulfate metabolism products such as AMP and Cys play important roles in Glc-responsive seedling growth through regulation of *AHL*.

Data presented here suggest that AtRZF1 is a negative regulator of AHL in response to Glc. We show that AHL is a PAP phosphatase linked to sulfate metabolism for mediating Glc response, although its molecular mechanisms have not been characterized completely yet. Here, in response to high Glc, AHL modulates the synthesis of AMP and Cys in sulfate metabolism and affects proline and ROS levels, leading to the Glc-induced response phenotype of early seedling stage (Supplementary Fig. S6). Additionally, Glc-induced sensitive phenotype of *pca17* treated with AMP showed a close to *atrzf1* phenotype, indicating a rescue of *pca17* by exogenously supplied AMP (Fig. 7). Therefore, AMP participates in many metabolism processes, including plant growth and high Glc response. Furthermore, expression profiling data of several Glc-upregulated genes (Fig. 4) suggested that AHL can amplify or repress the signal required for regulating the expression of Glc-inducible genes under high Glc condition. Thus, E3 ubiquitin ligase AtRZF1 give rise to high Glc-induced sensitive phenotype by suppressing AHL (Supplementary Fig. S6). Therefore, *atrzf1* mutant cannot disrupt the transmission of Glc signal to sulfate metabolism, which may affect both enhanced proline accumulation and reduced ROS production, thereby increasing early seedling growth under high Glc condition. Taken together, this proposed model demonstrates that AtRZF1-AHL coordinated regulation plays an important role in regulating Glc-mediated early seedling growth. Further studies may provide molecular links between Glc signaling and plant sulfate metabolism pathway. Interaction mechanisms between AtRZF1 and AHL merit further elucidation in future studies.

4. Materials and methods

4.1. Plant materials, growth, conditions, and Glc treatment

In this study, we used seeds of *Arabidopsis thaliana* (Col-0), *atrzf1*, *pca17*, and *AHL* transgenic lines including *AHL*-overexpressing (OE2-2, OE5-1), *ahl* RNAi (*ri2-3*, *ri5-2*), and complementary (Com4, Com9) lines previously described by Shin et al. (2019). *Arabidopsis* plants were grown under standard growth room conditions (22 °C, 16 h light/8 h dark, and 60% relative humidity). After 14-day-old *Arabidopsis* plants were treated with solution containing 6% Glc, samples were collected at 0, 3, 6, and 12 h. In each case, retrieved samples were quickly frozen in liquid nitrogen and then stored at −80 °C.

4.2. Analysis of GUS expression

Generation of *AHL* promoter $_{(PRO)}$-GUS constructs was determined as described previously (Shin et al., 2019). Histochemical staining for GUS expression in *AHL* $_{PRO}$-GUS transgenic lines (*AHL* $_{PRO}$-GUS 2–1, *AHL* $_{PRO}$-GUS 3-3) was carried out as reported previously (Jefferson et al., 1987). Seedling samples were placed in 100 mM sodium phosphate buffer (pH 7.0) containing 1 mM 5-bromo-4-chloro-3-indolyl-β-glucuronic acid (X-Gluc) and then incubated at 37 °C for 4 h. After clearing by 75% ethanol for overnight, seedling samples were photographed under a microscope.

4.3. Amino acids determination and AMP measurement

Pro content was estimated following method of Bates et al. (1973). Pro was isolated from 0.2 g of plant leaves by grinding in 2 mL of 3% sulfosalicylic acid. Then 200 μL of the preparation was reacted with 100 μL of ninhydrin reagent buffer for 1 h at 100 °C, cooled rapidly, and then centrifuged at 10,000 rpm for 10 min at 4 °C. This mixture was added with 500 μL of toluene and gently vortexed. Absorbance of toluene layer was measured at wavelength of 520 nm with a UV/VIS spectrophotometer (JASCO, Tokyo, Japan). Pro concentration was determined from a standard curve.

Cys content in *Arabidopsis* seedling plants was estimated by extracting 400 mg of leaves homogenized in 5% chilled perchloric acid, centrifuged at 10,000 rpm for 15 min at 4 °C following published method (Priya et al., 2016). The supernatant containing Cys was mixed with ninhydrin reagent and glacial acetic acid at equal volume (mL, 1: 1: 1). The reaction mixture was heated at 95 °C for 10 min and cooled rapidly. Its absorbance was then measured at 560 nm.

AMP was quantified as described previously (Chen et al., 2011). Extracted samples were analyzed using HPLC/ESI-MS (Shimadzu, Kyoto, Japan). HPLC conditions were: a Shiseido CAPCELL PAK C18 MG III column (100 mm × 3.0 mm I.D., 3 μm) (Shiseido, Tokyo, Japan), a flow rate of 0.8 mL/min (LC10AD, Shimadzu), and oven temperature of 35 °C (LC20A, Shimadzu). The sample was eluted using a gradient system including eluent A (5% acetonitrile and 10 mM *n*-hexylamine, pH 6.5) to eluent B (90% methanol and 10 mM ammonium acetate). The elution process was started with 100% eluent A, increasing to 100% eluent B for 15 min, and holding at 100% eluent B for 2 min. The mass spectrometer (negative ion mode) was set up to monitor *m/z* 345.85 → 79.05 for AMP with retention time for a second per transition. To obtain optimal mass spectrometer condition for AMP, the following system conditions were employed: ESI source voltage, 3.5 kV; detector voltage, 45 V; heat block temperature, 400 °C; and desolvation line temperature, 250 °C. Flow rates for nebulizing and drying gas were set at 3 L/min and 15 L/min, respectively. Argon collision gas was used at a 230-kPa pressure. Optimized collision energy for AMP was 40 eV. External standard of AMP was diluted to obtain various concentrations (0–67 μmol/L) for constructing a calibration curves by plotting peak areas with compound concentration.

4.4. DAB staining

The Glc-induced H_2O_2 accumulation was analyzed by soil or MS plate growing *Arabidopsis* seedling (Col-0) treated with 15% Glc because of the higher level of insensitive to Glc of Col-0 ecotype (Arenas-

Huertero et al., 2000). Hydrogen peroxide was detected by DAB staining following the method of Daudi and O'Brien (2012). Briefly, detached 5th-leaf of 5-week-old plants and 1-week-old seedling plants of WT, *atrzf1*, and *pca17* were transferred to 15% Glc for 12 h and 6 h, respectively. These samples were stained with 3,3′-diaminobenzidine (DAB) for 12 h. DAB was distained and chlorophyll was removed by a mixture bleach solution of ethanol, acid acetic, and glycerol (3:1:1).

Contributions of authors

The work presented here was carried out in collaboration between all authors; TV Nguyen and CS Kim designed research; TV Nguyen, MS Chung, and JS Chung performed research; TV Nguyen, MS Chung, JS Chung, and CS Kim analyzed data; TV Nguyen and CS Kim wrote the paper.

Conflicts of interest

The authors have no conflicts of interest relevant to this study to disclose.

Author contributions

We thank Dr. M-SC for technical assistance with HPLC analysis. CSK designed experiments and interpreted results. TVN and J-SC performed experiments and interpreted results.

Acknowledgements

This work was supported in part by a grant to C.S.K. from the Next-Generation BioGreen21 program (SSAC, PJ013171) funded by the Rural Development Administration. It was also supported by a grant (2018R1D1A1B07045242) of the Basic Science Research Program funded by the Ministry of Education, Science and Technology, Republic of Korea.

Appendix A. Supplementary data

Supplementary data to this article can be found online at https://doi.org/10.1016/j.plaphy.2019.09.019.

References

Alvarez, C., Calo, L., Romero, L.C., García, I., Gotor, C., 2010. An O-acetylserine(thiol) lyase homolog with L-cysteine desulfhydrase activity regulates cysteine homeostasis in *Arabidopsis*. Plant Physiol. 152, 656–669.

Anjum, N.A., Gill, R., Kaushik, M., Hasanuzzaman, M., Pereira, E., Ahmad, I., Tuteja, N., Gill, S.S., 2015. ATP-sulfurylase, sulfur-compounds, and plant stress tolerance. Front. Plant Sci. 6, 210.

Arenas-Huertero, F., Arroyo, A., Zhou, L., Sheen, J., Leon, P., 2000. Analysis of *Arabidopsis* glucose insensitive mutants, *gin5* and *gin6*, reveals a central role of the plant hormone ABA in the regulation of plant vegetative development by sugar. Genes Dev. 14, 2085–2096.

Bates, L.S., Waldren, R.P., Teare, I.D., 1973. Rapid determination of free proline for water-stress studies. Plant Soil 39, 205–207.

Chan, K.X., Wirtz, M., Phua, S.Y., Estavillo, G.M., Pogson, B.J., 2013. Balancing metabolites in drought: the sulfur assimilation conundrum. TIBS (Trends Biochem. Sci.) 18, 18–29.

Chen, H., Zhang, B., Hicks, L.M., Xiong, L., 2011. A nucleotide metabolite controls stress-responsive gene expression and plant development. PLoS One 6, e26661.

Cheng, W.H., Endo, A., Zhou, L., Penney, J., Chen, H.C., Arroyo, A., Leon, P., Nambara, E., Asami, T., Seo, M., Koshiba, T., Sheen, J., 2002. A unique short-chain dehydrogenase/reductase in *Arabidopsis* glucose signaling and abscisic acid biosynthesis and functions. Plant Cell 14, 2723–2743.

Coello, P., Hey, S.J., Halford, N.G., 2011. The sucrose non-fermenting-1-related (SnRK) family of protein kinases: potential for manipulation to improve stress tolerance and increase yield. J. Exp. Bot. 62, 883–893.

Daudi, A., O'Brien, J.A., 2012. Detection of hydrogen peroxide by DAB staining in *Arabidopsis* leaves. BIO-PROTOCOL 2, e263.

Davies, J.P., Yildiz, F.H., Grossman, A.R., 1999. Sac3, an Snf1-like serine/threonine kinase that positively and negatively regulates the responses of Chlamydomonas to sulfur limitation. Plant Cell 11, 1179–1190.

Dixon, D.P., Lapthorn, A., Edwards, R., 2002. Plant glutathione transferases. Genome Biol. 3 reviews3004.1-3004.10.

Dominguez-Solis, J.R., Lopez-Martin, M.C., Ager, F.J., Ynsa, M.D., Romero, L.C., Gotor, C., 2004. Increased cysteine availability is essential for cadmium tolerance and accumulation in *Arabidopsis thaliana*. Plant Biotechnol. J. 2, 469–476.

Dunand, C., Crèvecoeur, M., Penel, C., 2007. Distribution of superoxide and hydrogen peroxide in *Arabidopsis* root and their influence on root development: possible interaction with peroxidases. New Phytol. 174, 332–341.

Estavillo, G.M., Crisp, P.A., Pornsiriwong, W., Wirtz, M., Collinge, D., Carrie, C., Giraud, E., Whelan, J., David, P., Javot, H., Brearley, C., Hell, R., Marin, E., Pogson, B.J., 2011. Evidence for a SAL1-PAP chloroplast retrograde pathway that functions in drought and high light signaling in *Arabidopsis*. Plant Cell 23, 3992–4012.

Graham, I.A., Denby, K.J., Leaver, C.J., 1994. Carbon catabolite repression regulates glyoxylate gene expression in cucumber. Plant Cell 4, 761–772.

Hayat, S., Hayat, Q., Alyemeni, M.N., Wani, A.S., Pichtel, J., Ahmad, A., 2012. Role of proline under changing environments: a review. Plant Signal. Behav. 7, 1456–1466.

Jang, J.C., Leon, P., Zhou, L., Sheen, J., 1997. Hexokinase as a sugar sensor in higher plants. Plant Cell 9, 5–19.

Jefferson, R.A., Klass, M., Wolf, N., Hirsh, D., 1987. Expression of chimeric genes in *Caenorhabditis elegans*. J. Mol. Biol. 1, 41–46.

Ju, H.W., Min, J.H., Chung, M.S., Kim, C.S., 2013. The *atrzf1* mutation of the novel RING-type E3 ubiquitin ligase increases proline contents and enhances drought tolerance in *Arabidopsis*. Plant Sci. 203–204, 1–7.

Kim, A.R., Min, J.H., Lee, K.H., Kim, C.S., 2017. PCA22 acts as a suppressor of *atrzf1* to mediate proline accumulation in response to abiotic stress in *Arabidopsis*. J. Exp. Bot. 68, 1797–1809.

Kuzniak, E., Sklodowska, M., 2005. Compartment-specific role of the ascorbate-glutathione cycle in the response of tomato leaf cells to *Botrytis cinerea* infection. J. Exp. Bot. 56, 921–933.

León, P., Sheen, J., 2003. Sugar and hormone connections. Trends Plant Sci. 8, 110–116.

Li, Y., Lee, K.K., Walsh, S., Smith, C., Hadingham, S., Sorefan, K., Cawley, G., Bevan, M.W., 2006. Establishing glucose- and ABA-regulated transcription networks in *Arabidopsis* by microarray analysis and promoter classification using a relevance vector machine. Genome Res. 16, 414–427.

Mendoza-Cozatl, D.G., Jobe, T.O., Hauser, F., Schroeder, J.I., 2011. Long-distance transport, vacuolar sequestration, tolerance, and transcriptional responses induced by cadmium and arsenic. Curr. Opin. Plant Biol. 14, 554–562.

Miao, H., Cai, C., Wei, J., Huang, J., Chang, J., Qian, H., Zhang, X., Zhao, Y., Sun, B., Wang, B., Wang, Q., 2016. Glucose enhances indolic glucosinolate biosynthesis without reducing primary sulfur assimilation. Sci. Rep. 6, 31854.

Min, J.H., Ju, H.W., Yoon, D., Lee, K.H., Lee, S., Kim, C.S., 2017. *Arabidopsis* Basic Helix-Loop-Helix 34 (bHLH34) is involved in glucose signaling through binding to a GAGA *cis*-element. Front. Plant Sci. 8, 2100.

Noctor, G., Mhamdi, A., Chaouch, S., Han, Y., Neukermans, J., Marquez-Garcia, B., Foyer, C.H., 2012. Glutathione in plants: an integrated overview. Plant Cell Environ. 35, 454–484.

Pornsiriwong, W., Estavillo, G.M., Chan, K.X., Tee, E.E., Ganguly, D., Crisp, P.A., Phua, S.Y., Zhao, C., Qiu, J., Park, J., Yong, M.T., Nisar, N., Yadav, A.K., Schwessinger, B., Rathjen, J., Cazzonelli, C.I., Wilson, P.B., Gilliham, M., Chen, Z.H., Pogson, B.J., 2017. A chloroplast retrograde signal, 3'-phosphoadenosine 5'-phosphate, acts as a secondary messenger in abscisic acid signaling in stomatal closure and germination. eLife 6, e23361.

Price, J., Laxmi, A., St Martin, S.K., Jang, J.C., 2004. Global transcription profiling reveals multiple sugar signal transduction mechanisms in *Arabidopsis*. Plant Cell 16, 2128–2150.

Priya, M., Raj, A.S., Muthukumar, P.V., Bharathiraja, B., 2016. Experimental study on biochemical and physiological adaptation of mercury accumulation and tolerance in *Clitoria ternatea* L. JCHPS 9, 298–303.

Rea, P.A., 2012. Phytochelatin synthase: of a protease a peptide polymerase made. Physiol. Plant. 145, 154–164.

Rolland, F., Baena-Gonzalez, E., Sheen, J., 2006. Sugar sensing and signaling in plants: conserved and novel mechanisms. Annu. Rev. Plant Biol. 57, 675–709.

Romero, L.C., Aroca, M.Á., Laureano-Marín, A.M., Moreno, I., García, I., Gotor, C., 2014. Cysteine and cysteine-related signaling pathways in *Arabidopsis thaliana*. Mol. Plant 7, 264–276.

Sakr, S., Wang, M., Dédaldéchamp, F., Perez-Garcia, M.D., Ogé, L., Hamama, L., Atanassova, R., 2018. The sugar-signaling hub: overview of regulators and interaction with the hormonal and metabolic network. Int. J. Mol. Sci. 19, 2506.

Sami, F., Hayat, S., 2019. Effect of glucose on the morpho-physiology, photosynthetic efficiency, antioxidant system, and carbohydrate metabolism in *Brassica juncea*. Protoplasma 256, 213–226.

Shin, D.J., Min, J.H., Nguyen, T.V., Kim, Y.M., Kim, C.S., 2019. Loss of *Arabidopsis Halotolerance 2-like* (AHL), a 3′- phosphoadenosine-5′-phosphate phosphatase, suppresses insensitive response of *Arabidopsis thaliana ring zinc finger 1* (*atrzf1*) mutant to abiotic stress. Plant Mol. Biol. 99, 363–377.

Strizhov, N., Abraham, E., Okresz, L., Blickling, S., Zilberstein, A., Schell, J., Koncz, C., Szabados, L., 1997. Differential expression of two *P5CS* genes controlling proline accumulation during salt-stress requires ABA and is regulated by *ABA1, ABI1* and *AXR2* in *Arabidopsis*. Plant J. 12, 557–569.

Szabados, L., Savouré, A., 2010. Proline: a multifunctional amino acid. Trends Plant Sci. 15, 89–97.

Takahashi, H., Kopriva, S., Giordano, M., Saito, K., Hell, R., 2011. Sulfur assimilation in photosynthetic organisms: molecular functions and regulations of transporters and assimilatory enzymes. Annu. Rev. Plant Biol. 62, 157–184.

Yu, Q., Tian, H., Yue, K., Liu, J., Zhang, B., Li, X., Ding, Z., 2016. A P-Loop NTPase regulates quiescent center cell division and distal stem cell identity through the regulation of ROS homeostasis in *Arabidopsis* root. PLoS Genet. 12, e1006175.